University of Dundee

0.5 billion events per second time correlated single photon counting using CMOS SPAD arrays

Krstajic, Nikola; Poland, Simon; Levitt, James; Walker, Richard; Erdogan, Ahmet T.; Ameer-Beg, Simon; Henderson, Robert K

.5 billion events per second time correlated single photon counting using CMOS SPAD arrays

Nikola Krstajić,[1,2,*] **Simon Poland,**[3] **James Levitt,**[3] **Richard Walker,**[1,4] **Ahmet Erdogan,**[1] **Simon Ameer-Beg,**[3] **Robert K. Henderson**[1]

[1]*Institute for Integrated Micro and Nano Systems, School of Engineering, University of Edinburgh, Edinburgh, UK;*
[2]*EPSRC IRC "Hub" in Optical Molecular Sensing & Imaging, MRC Centre for Inflammation Research, Queen's Medical Research Institute, 47 Little France Crescent, Edinburgh, UK;*
[3]*Division of Cancer Studies & Randall Division of Cell and Molecular Biophysics, Guy's Campus, Kings College, London, UK;*
[4]*Photon Force Ltd, Edinburgh*
Corresponding author: n.krstajic@physics.org

We present a digital architecture for fast acquisition of time correlated single photon counting (TCSPC) events from a 32×32 CMOS SPAD array (Megaframe) to the computer memory. Custom firmware was written to transmit event codes from 1024 TCSPC-enabled pixels for fast transfer of TCSPC events. Our 1024 channel TCSPC system is capable of acquiring up to 0.5×10^9 TCSPC events per second with 16 histogram bins spanning 14 ns width. Other options include 320×10^6 TCSPC events per second with 256 histogram bins spanning either 14 ns or 56 ns time window. We present a wide-field fluorescence microscopy setup demonstrating fast fluorescence lifetime data acquisition. To the best of our knowledge, this is the fastest direct TCSPC transfer from a single photon counting device to the computer to date. © 2015 Optical Society of America

Time correlated single photon counting (TCSPC) is the most accurate technique available for determining fluorescence decays down to sub-nanosecond time ranges. The technique originated in nuclear physics where scintillation decay curves provided clues about the nuclear particles being detected by the scintillating crystal [1]. Over time, TCSPC has expanded into chemistry [2] and a range of biomedical applications [3] including fluorescence lifetime imaging (FLIM) [4,5]. Printed circuit board (PCB) level electronics integration enabled widespread use of TCSPC since the early '90s when commercial suppliers provided bespoke systems for a range of applications from quantum optics to tissue imaging. We believe that the next technological push will involve integrating single photon detection, timing and processing circuitry on a single semiconductor die. The best contender for this leap is the standard complementary metal oxide semiconductor (CMOS) technology [6], because standard CMOS has already been the key driver in global electronics miniaturization.

A number of CMOS single photon avalanche detector (SPAD) sensors have achieved low noise, high frame rate and scalability needed for fluorescence imaging applications [7,8]. CMOS SPAD imaging sensors enable highly parallelized TCSPC, but at the same time present a serious data bottleneck. The CMOS SPAD sensor used in this study is 32 × 32 pixel, 55 ps time resolution, 10 bit time-to-digital converter (TDC), 56 ns time window, Megaframe (MF32) sensor [7,8]. Whilst the fill factor of the MF32 sensor used is low (1.5%), our previous work demonstrates optical fill factor amplification to 100% [9,10] by generating 64 fluorescence beamlets which are imaged onto the active area of the SPAD (fill factor amplification is not used in the work presented here). The MF32 interface to the field programmable gate array (FPGA) is limited to 500000 frames per second (fps) and the transfer of this data to the computer has not been optimised. This manuscript addresses the data bottleneck challenge by achieving optimal count rates from the sensor to the computer memory via FPGA and the universal serial bus 3 (USB3).

To the best of our knowledge, we demonstrate the best TCSPC count rates to date. Prior work [11] achieved 80 million counts per second (often referred to as timestamps or time-tags) (Mcps) without taking into account pile-up effects in their lifetime determination. In present work we demonstrate 500 Mcps. This value is close to acceptable limit for counts in terms of pulse pile-up (1% for a laser rep rate of 50MHz). Such count rate is likely to cater for larger sensors since low light widefield fluorescence detection usually acquires 1000-5000 counts per second [12] meaning that a 100 × 100 pixel TCSPC sensor would work well (assuming 100% fill factor). The results presented here are directly applicable to multi-beam scanning required for ultrafast FLIM applications [13].

The measured TCSPC events need to be passed from the sensor to the FPGA, and then from the FPGA to the computer, see Fig. 1. As shown on Fig. 1. the interface to MF32 sensor consists of clocking the LINECLK line at 8MHz. This clock places data on the 64 bit DATA_TDC parallel bus. The readout reads two lines of 10 bit TDC values from the sensor for each LINECLK cycle. The DATA_SAMPLE_CLK is set to 80MHz which enables the sampling of the 10 bit TDC value over 10 clock cycles to fit the LINECLK 8MHz rate. 640 bits (64 pixels with 10 bit TDC values) are processed by the MF32 interface module on the

FPGA. For best performance, 64 × 10 bit TDC values are compressed to 64 × 4 bit TDC values losing some time resolution, but allowing unprecedented TCSPC event rate. The resulting 256 bits (64 pixels with 4 bit TDC values) need to be sent via USB3 every 125 μs. Total data throughput required is thus 256 megabytes per second (MB/s). USB3 bus has maximum data rate of 300-340 MB/s, so it gives ample room to fit 0.5 billion events per second. USB3 bus is not real-time, so a first in first out (FIFO) buffer is needed to allow for communications to be smooth. 128 kilobytes (KB) FIFO buffer was implemented with 128 bit input (FIFO_DATA_IN) and 32 bit output (FIFO_DATA_OUT). The manufacturer of the PCB (Opal Kelly) provides a dedicated 32 bit bus on the FPGA and FIFO_DATA_OUT is channeled via USB3.

The timing diagram shown in Fig. 2. further illustrates the clocking frequencies of the data path. Data from the MF32 sensor is fed into the FIFO over 128 bit wide bus at 32 MHz. USB3 data is clocking 32 bits of data at 100MHz thus allowing up to 400 MB/s in principle. However, the USB3 protocol overheads and delays on the either the PC or embedded side may hold up the communications, so sustained 300-340MB/s is usually achievable on most PCs with USB3 link.
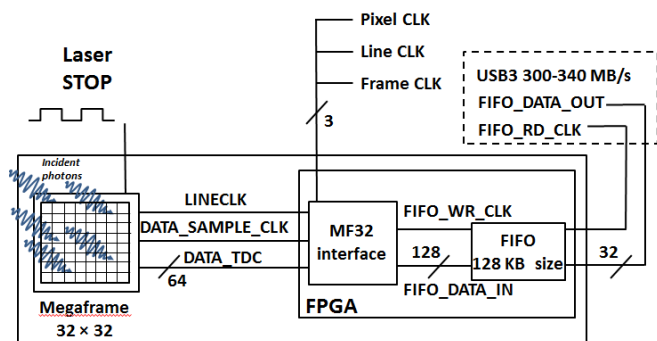

Fig. 1. MF32 embedded system architecture illustrating the FPGA's role in channeling data from the MF32 to computer via the USB3 serial bus. Laser scanning microscopy is enabled via trigger signals (PIXEL, LINE and FRAME clocks) while the laser STOP halts the TDC.
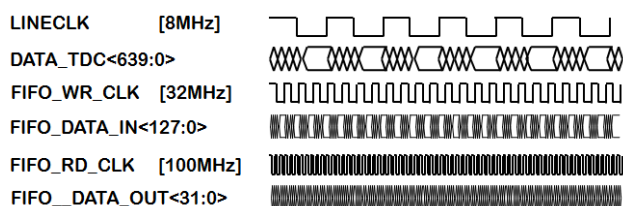

Fig. 2. Timing diagram of the main clock and data signals.

The TDC in MF32 is 10 bits long and the histogram time window spans 0 to 1023 bins, with each having 55 ps time resolution resulting in time window of 56 ns. The time resolution of 55 ps can be tuned between 50 ps and 100 ps by manipulating sensor settings [14]. Also, depending on the repetition rate of the laser, the histogram time window of interest might be shorter than the time window available (repetition rate >17.86 MHz for 56 ns time window). This allows TDC time-correlated event value to be processed on FPGA without loss of information. As shown in Fig. 3., the expected fluorescence lifetimes in the given specimen need to be considered. The probe with slowly decaying fluorescence (shown in Fig. 3.) requires a full 56 ns time window while the fast decay requires 14 ns and therefore only the bottom 8 bits of the TDC. This is the situation with fast repetition rate mode-locked lasers such as Ti:Sapphire and pulsed laser diodes where the repetition rate can be >75 MHz,. The 8 bit TDC covering the 0 to 14 ns time window is appropriate in this case and the compression is lossless in terms of time resolution.

A wide-field FLIM setup was built to illustrate fast TCSPC event collection direct to computer memory (see Fig. 4). *Convallaria majalis*

rhizome stained with acridine orange (As-812z, Medical Science Media, Australia) was used as a test specimen. A pulsed laser (485 nm, 64ps, Hamamatsu plp10 laser driver) was coupled to a 400 μm diameter multimode fiber and used to illuminate the slide via a dichroic beamsplitter (Semrock,, FF499-Di01-25x36) and infinity-corrected microscope objective (Thorlabs, RMS10X). Fluorescence from the slide was imaged onto MF32 and color CCD (PCO pixelfly usb, Bayer color filter, PCO Gmbh) cameras simultaneously after passing it through emission filter (Semrock FF01-530/43-25) and beamsplitting the signal. The pulsed laser was used at the maximum 100 MHz repetition rate. The CMOS SPAD sensor was controlled using custom software developed in the LabVIEW 2014 graphical programming environment (National Instruments). We use a USB3 enabled Opal Kelly board XEM6310-LX150 which contains a Spartan 6 FPGA (Xilinx, USA). Instrument response function (IRF) was acquired by placing a solution of Ludox (Sigma Aldrich) in the position of specimen. Emission filter was removed and the neutral density filter was added to the emission path to reduce the intensity of backscattered light (dichroic used passes ~0.1% at 485 nm excitation wavelength). As described before, each pixel has a separate IRF acquired and this IRF is used for lifetime estimation of the respective pixel.
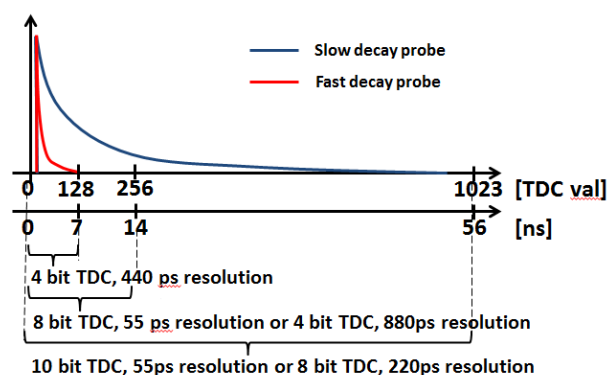

Fig. 3. The time window is adjusted to the TDC word to enable compression. 10 bit TDC covers 56 ns time window at 55ps time resolution or 8 bit TDC covers the same range at 220 ps time resolution.
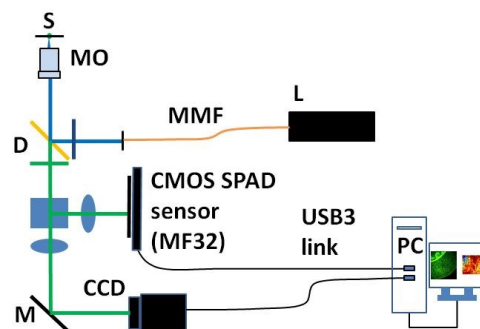

Fig. 4. Wide-field FLIM setup. Pulsed laser (L) is coupled into 400 μm multimode fiber (MMF) and used to illuminate sample (S) via microscope objective (MO) and dichroic (D). Fluorescence from the sample is split into two detectors, CCD and CMOS SPAD sensor. Data from both sensors is simultaneously uploaded to the computer.

An example of wide-field microscopy and FLIM images acquired by the setup described above is shown in Fig. 5. The three square regions shown in Fig. 5 (image to the left) are the regions focused onto MF32. MF32 was mounted on XY stage to manually move the field of view (FOV) to allow selection of multiple regions within FOV. Due to small resolution of MF32, we opted to adjust the image magnification so that MF32 shows a smaller region of the field of view than is available to the

CCD. Three images on the right of Fig. 5. are FLIM images. The lifetime was extracted using iterative reconvolution with Levenberg-Marquard fitting using custom Matlab scripts derived from DecayFit 1.3 [15,16]. The FLIM images shown in Fig. 5. were acquired in 3s at 320 Mcps with an 8 bit TDC covering the 14 ns time window and a 100 MHz laser repetition rate. Out of 320Mcps, 11×10^6 events were non-zero values fed into histograms. Over 3s this resulted in 33000 events per pixel on average. The transfer is organized on frame per frame basis, so if no photon is detected in a given frame's exposure time then the value for the pixel is written as 0. Pile-up artefact is avoided by assuring that the frame rate is <1% of the laser repetition rate. With higher laser power, improved optics and fill factor improvement [9,10,13] this value will easily scale to 500 Mcps of photon events. We verified full data rates by acquiring the IRF at maximum data rates with >96% non-zero events. The FLIM images will also improve in clarity once full pixel timing calibration is applied, such as integral non-linearity and differential non-linearity corrections [13]. The sample decay from the FLIM image is shown in Fig. 6. The time window is 14 ns wide and 8 bit TDC time-correlated event were used at 55ps time resolution. Decay pre-pulse appearing at ~2 ns in Fig. 6. is related to the optical setup (either specimen or emission path). Pre-pulse does not appear on any of the IRFs acquired.

We tested data rates under a variety of TDC configurations and the results are outlined in Table 1. We were able to maintain 320 MB/s data rate securing count rates of 500 Mcps in 4 bit TDC. The upper limit is the current readout rate of MF32 from FPGA which is 500000 frames per second. We succeeded in maintaining this rate for the 4 bit TDC size and 4 bit single photon count frames. Our tests were performed on $30 \times .1$ s acquisitions. We interleave acquisitions with histogramming to reduce loading on the computer memory. For each .1s of acquisition, histogramming takes approximately 1s. Our aim is to reduce this by deploying faster histogramming routines, possibly involving graphics processing units (GPUs). Our extensive tests show that 320 MB/s is broadly maintained for 1 hour tests, standard deviation of the data rate variation is 6 MB/s. We found that USB3 cabling plays a crucial role. The quality of cables varies and we found that Point Grey Research ACC-01-2300 3m USB3 cable to give more consistent results. As USB3 becomes more adopted cabling is unlikely to be an issue. Computer architecture deployed is also important. 64 bit operating system should be used with minimum 16 GB dynamic memory.
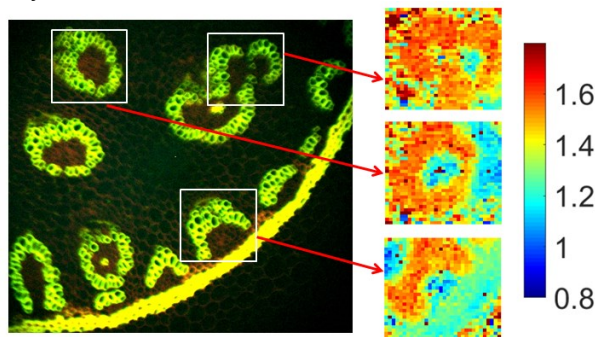

Fig. 5. *Convallaria majalis* fluorescence intensity image from the CCD (50 ms integration time) is shown on the left and three FLIM images to the right come from white squares in the color CCD image. The MF32 FLIM image data was acquired in 3 s.

As expected, the decay for 4 bit TDC transfer is coarser than the decay for 10 bit TDC transfer, as shown in Fig. 7. It should also be noted that for 100 MHz repetition rate, 8 bit TDC for 14 ns time window has the same coarseness as full 10 bit TDC for 56 ns time window. 4 bit TDC transfer has higher number of photons per bin, because 16 bins cover 14 ns time window as opposed photon counts being spread over 256 bins in 8 bit TDC transfer over the same 14 ns time window. So despite the loss in time resolution, one may obtain a decay curve sooner in 4 bit TDC transfer. The problem is more complex, because

both the time resolution and the number of photon events in the histogram affect the lifetime estimation accuracy. Prior work shows promising prospects for histogramming with similar coarseness to 4 bit TDC transfer [17,18].

We have demonstrated ultra-fast TCSPC event code transfer from the CMOS SPAD array. As mentioned above, our aim is to deploy this sensor in a variety of physics, biology and pre-clinical applications. It is important to note that the most beneficial implementation for MF32 will be the one which amplifies the fill factor, as this ensures low dark count rate (DCR) due to small SPAD area whilst reducing photobleaching and maintaining a high count rate. Also, the high count rates demonstrated here indicate what should be expected from future TCSPC sensor cameras over USB3 or similar links. Lastly, top range FPGA architectures have more than 50MB of static RAM available on-chip (at the time of writing) allowing fast parallelized read-modify-write histogramming of at least 25000 TCSPC pixels.
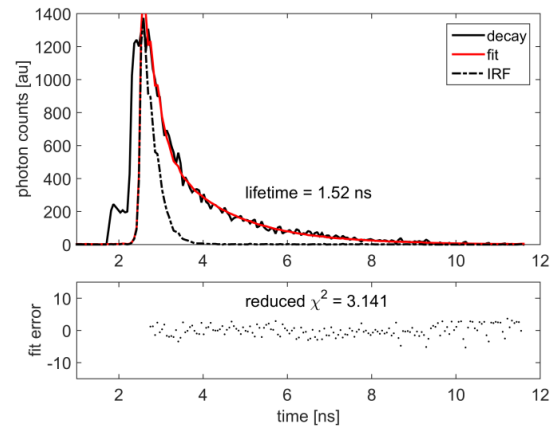

Fig. 6. Fluorescence decay curve from FLIM image and associated reduced χ^2 error.

TCSPC event code size	Time window size	Data rate	Achieved count rate
10 bit	56 ns	320 MB/s	160 Mcps
8 bit	56 ns	320 MB/s	310 Mcps
8 bit	14 ns	320 MB/s	310 Mcps
4 bit	14 ns	260 MB/s	500 Mcps

Table 1. Data rates and count rates for 10 bit, 8 bit and 4 bit TDC modes.
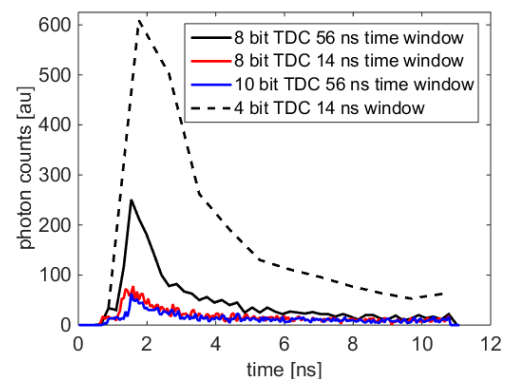

Fig. 7. Decay curves for a sample pixel for variety of TDC sizes.

References

1. L. M. Bollinger and G. E. Thomas, "Measurement of the Time Dependence of Scintillation Intensity by a Delayed-Coincidence Method," Review of Scientific Instruments **32**, 1044–1050 (1961).
2. D. V. O'Connor and D. Phillips, *Time-Correlated Single Photon Counting* (Academic Press, 1984).
3. W. Becker, *Advanced Time-Correlated Single Photon Counting Techniques*, illustrated edition (Springer, 2005).
4. L. Marcu, P. M. W. French, and D. S. Elson, eds., *Fluorescence Lifetime Spectroscopy and Imaging: Principles and Applications in Biomedical Diagnostics*, 1 edition (CRC Press, 2014).
5. K. Suhling, L. M. Hirvonen, J. A. Levitt, P.-H. Chung, C. Tregido, A. le Marois, D. A. Rusakov, K. Zheng, S. Ameer-Beg, S. Poland, S. Coelho, and R. Dimble, "Fluorescence Lifetime Imaging (FLIM): Basic Concepts and Recent Applications," in *Advanced Time-Correlated Single Photon Counting Applications*, W. Becker, ed., Springer Series in Chemical Physics No. 111 (Springer International Publishing, 2015), pp. 119–188.
6. E. Charbon, "Single-photon imaging in complementary metal oxide semiconductor processes," Philosophical Transactions of the Royal Society of London A: Mathematical, Physical and Engineering Sciences **372**, (2014).
7. J. Richardson, R. Walker, L. Grant, D. Stoppa, F. Borghetti, E. Charbon, M. Gersbach, and R. K. Henderson, "A 32 x32 50ps resolution 10 bit time to digital converter array in 130nm CMOS for time correlated imaging," in *IEEE Custom Integrated Circuits Conference, 2009. Cicc '09* (2009), pp. 77 –80.
8. J. Richardson, E. A. G. Webster, L. A. Grant, and R. K. Henderson, "Scaleable Single-Photon Avalanche Diode Structures in Nanometer CMOS Technology," IEEE Transactions on Electron Devices **58**, 2028–2035 (2011).
9. S. P. Poland, N. Krstajić, R. D. Knight, R. K. Henderson, and S. M. Ameer-Beg, "Development of a doubly weighted Gerchberg–Saxton algorithm for use in multibeam imaging applications," Opt. Lett. **39**, 2431–2434 (2014).
10. S. P. Poland, N. Krstajić, S. Coelho, D. Tyndall, R. J. Walker, V. Devauges, P. E. Morton, N. S. Nicholas, J. Richardson, D. D.-U. Li, K. Suhling, C. M. Wells, M. Parsons, R. K. Henderson, and S. M. Ameer-Beg, "Time-resolved multifocal multiphoton microscope for high speed FRET imaging in vivo," Opt. Lett. **39**, 6013–6016 (2014).
11. J. L. Rinnenthal, C. Börnchen, H. Radbruch, V. Andresen, A. Mossakowski, V. Siffrin, T. Seelemann, H. Spiecker, I. Moll, J. Herz, A. E. Hauser, F. Zipp, M. J. Behne, and R. Niesner, "Parallelized TCSPC for Dynamic Intravital Fluorescence Lifetime Imaging: Quantifying Neuronal Dysfunction in Neuroinflammation," PLoS ONE **8**, e60100 (2013).
12. Q. Zhao, I. T. Young, and J. G. S. de Jong, "Photon budget analysis for fluorescence lifetime imaging microscopy," J. Biomed. Opt **16**, 086007–086007 (2011).
13. S. P. Poland, N. Krstajić, J. Monypenny, S. Coelho, D. Tyndall, R. J. Walker, V. Devauges, J. Richardson, N. Dutton, P. Barber, D. D.-U. Li, K. Suhling, T. Ng, R. K. Henderson, and S. M. Ameer-Beg, "A high speed multifocal multiphoton fluorescence lifetime imaging microscope for live-cell FRET imaging," Biomedical Optics Express **6**, 277 (2015).
14. N. Krstajić, S. Poland, D. Tyndall, R. Walker, S. Coelho, D. D. Li, J. Richardson, S. Ameer-Beg, and R. Henderson, "Improving TCSPC data acquisition from CMOS SPAD arrays," in (2013), Vol. 8797, pp. 879709–879709–8.
15. S. Preus, K. Kilså, F.-A. Miannay, B. Albinsson, and L. M. Wilhelmsson, "FRETmatrix: a general methodology for the simulation and analysis of FRET in nucleic acids," Nucl. Acids Res. gks856 (2012).
16. S. Preus, "DecayFit - Fluorescence Decay Analysis Software 1.3, FluorTools, www.fluortools.com," (2014).
17. M. Köllner and J. Wolfrum, "How many photons are necessary for fluorescence-lifetime measurements?," Chemical Physics Letters **200**, 199–204 (1992).
18. C. J. de Grauw and H. C. Gerritsen, "Multiple Time-Gate Module for Fluorescence Lifetime Imaging," Appl. Spectrosc., AS **55**, 670–678 (2001).